

Physics at ELFE¹

Paul Hoyer

Nordita

Blegdamsvej 17, DK-2100 Copenhagen Ø, Denmark

Abstract

I review some central physics opportunities at the 15...30 GeV continuous beam electron accelerator ELFE, proposed to be built in conjunction with the DESY linear collider. Our present detailed knowledge of single parton distributions in hadrons and nuclei needs to be supplemented by measurements of compact valence quark configurations, accessible through hard exclusive scattering, and of compact multiparton subsystems which contribute to semi-inclusive processes. Cumulative ($x > 1$, $x_F > 1$) processes in nuclei measure short-range correlations between partons belonging to different nucleons in the same nucleus. The same configurations may give rise to subthreshold production of light hadrons and charm. The challenges of understanding high energy charmonium production indicate that charmonium will be a sensitive probe of color dynamics at ELFE. At low energies, charmonium forms inside the target nucleus, allowing a determination of $c\bar{c}$ bound state interactions in nuclear matter.

¹Based on talks given at the meeting on *Future Electron Accelerators and Free Electron Lasers*, Uppsala, April 25-26, 1996 and at the *Second ELFE Workshop*, Saint Malo, September 23-27, 1996. Work supported in part by the EU/TMR contract ERB FMRX-CT96-0008.

1 Introduction

The ELFE@DESY project aims at utilizing a future DESY linear electron collider [1] to accelerate electrons to 15...30 GeV and then use the HERA electron ring to stretch the collider bunches into an intense ($30 \mu\text{A}$) continuous extracted beam [2]. Polarized electrons will be scattered from both light and heavy fixed targets, with luminosities in the $\mathcal{L} = 10^{35} \dots 10^{38} \text{ cm}^{-2}\text{s}^{-1}$ range. In this talk I discuss some of the central physics issues that can be addressed with this type of accelerator. Since ELFE experiments are many years in the future I shall concentrate on questions related to basic descriptions of the structure of matter at the $\mathcal{O}(0.1 \text{ fm})$ scale in terms of QCD. These questions will remain of fundamental interest and require the capabilities of an accelerator like ELFE.

Table 1. **Features and opportunities of an ELFE accelerator.**

Features	Opportunities
High luminosity $\mathcal{L} \sim 10^{35} \dots 10^{38} \text{ cm}^{-2}\text{s}^{-1}$	Study rare configurations of target wave function
Energy $E = 15 \dots 30 \text{ GeV}$	Perturbative QCD Resolution of $\mathcal{O}(0.1 \text{ fm})$ Charm production
High duty factor $\sim 90\%$	Event reconstruction
Good energy resolution $\Delta E/E \simeq 10^{-3}$	Exclusive reactions Inclusive reactions at high x
Polarization	Amplitude reconstruction Spin systematics of QCD

In Table 1 I list the main features of the ELFE accelerator, and the opportunities that they provide. Compared to existing electron and muon beams, the advantages of ELFE are in luminosity (compared to the muon beams at CERN and Fermilab), in duty factor (compared to SLAC) and in energy (compared to TJNAF). Competitive ELFE experiments will rely on a combination of these strong features. The HERMES experiment at DESY works in the same energy range but at a lower luminosity and duty factor compared to ELFE. HERMES will prepare the ground for ELFE physics, together with experiments at TJNAF in the U.S., GRAAL in Grenoble and the lower energy electron facilities ELSA (Bonn) and MAMI (Mainz).

As I shall discuss below, an important part of physics at ELFE will deal with exclusive reactions, or with inclusive reactions at large values of Bjorken $x = Q^2/2m\nu$. The energy range of 15...30 GeV is actually optimal for such studies, as seen from the following argument. The inclusive deep inelastic cross-section scales (up to logarithmic terms) in the virtuality Q^2 and energy ν of the photon like

$$\frac{d^2\sigma_{DIS}}{dQ^2 dx} \propto \frac{1}{Q^4} F(x) \quad (1)$$

Exclusive processes are still more strongly suppressed at large Q^2 , eg,

$$\frac{d\sigma}{dQ^2}(ep \rightarrow ep) \propto \frac{F_p^2(Q^2)}{Q^4} \propto \frac{1}{Q^{12}} \quad (x = 1) \quad (2)$$

Typically we want to reach at least $Q^2 = \mathcal{O}(10 \text{ GeV}^2)$ to be able to use perturbative QCD (PQCD) and to have a resolution of $\mathcal{O}(0.1 \text{ fm})$. This implies $\nu = \mathcal{O}(5 \text{ GeV})$ at large $x \simeq 1$. At ELFE, such energies correspond to the photon taking a moderate fraction $y = \nu/E_e \simeq 0.15 \dots 0.3$ of the electron energy, which is practical for measurements. This may be contrasted with the situation at HERA, which is equivalent to a fixed target experiment with an electron energy $E_e \simeq 50000 \text{ GeV}$. A photon with energy $\nu = 5 \text{ GeV}$ would at HERA correspond to $y \simeq 0.0001$. It is clearly very difficult to measure the large x , moderate Q^2 region at HERA, but it is the natural territory of an accelerator in the ELFE energy range.

In the following I shall discuss three aspects of physics at ELFE which relate to basic issues in QCD:

- *Wave function measurements.* Most of our present knowledge of hadron and nuclear wave functions stems from hard inclusive scattering, which measures single parton distributions. The phenomenology of hard exclusive scattering, which is sensitive to compact valence quark configurations, is still in its infancy. Although considerable progress may be expected in this field in the coming years, the measurements are so demanding that an accelerator with ELFE's capabilities is sorely needed. On the theoretical front, we still do not have a full understanding of which properties of the wave function are in principle measurable in hard scattering. It seems plausible that semi-inclusive processes can be used to measure configurations where a subset of partons are in a compact configuration, while the others are summed over.
- *Short range correlations in nuclei.* Scattering which is kinematically forbidden for free nucleon targets has been experimentally observed, and includes DIS at $x > 1$, hadron production at Feynman $x_F > 1$ and subthreshold production processes. Such scattering requires short range correlations between partons in more than one nucleon, and thus gives information about unusual, highly excited nuclear configurations.

- *Charm production near threshold*¹. Production close to threshold requires efficient use of the target energy and hence favors compact target configurations. Heavy quarks are created in a restricted region of space-time, where perturbative calculations are reliable. Both features conspire to make the production of charm near threshold a sensitive measure of new physics, including unusual target configurations and higher twist contributions. The ELFE accelerator will work in the region of charm threshold ($E_\gamma \simeq 9$ GeV) and provide detailed information about both charmonium and open charm production.

The above selection of physics topics is obviously far from complete. I refer to earlier presentations of ELFE physics [3] as well as to the review by Brodsky [4] for further discussions of these and other aspects of QCD phenomenology. In particular, I shall not cover here the important and topical area of color transparency, but refer to recent reviews [5] and references therein.

2 Wave function measurements

2.1 Inclusive Deep Inelastic Scattering

Our most precise knowledge of nucleon (and nuclear) structure is based on deep inelastic lepton scattering (DIS), $\ell N \rightarrow \ell' X$, and related hard inclusive reactions. As is well-known, DIS measures the product of a parton-level subprocess cross-section $\hat{\sigma}$ and a target structure function F . Thus, schematically and at lowest order in the strong coupling α_s ,

$$\frac{d^2\sigma(eN \rightarrow eX)}{dQ^2 dx} = \hat{\sigma}(eq \rightarrow eq) F_{q/N}(x, Q^2) [1 + \mathcal{O}(\alpha_s)] \quad (3)$$

The structure functions $F_{q/N}$ have been measured over an impressive range in x and Q^2 , covering $.0001 \lesssim x \lesssim 1$ and $1 \lesssim Q^2 \lesssim 10000$ GeV². Their logarithmic Q^2 -dependence (‘scaling violations’) predicted by QCD has been tested, and their ‘universality’ verified, *ie*, the same structure functions describe other hard inclusive reactions such as $pp \rightarrow jet + X$, $\pi^- p \rightarrow \mu^+ \mu^- + X$ and $pp \rightarrow \gamma + X$. The many detailed measurements and successful cross-checks have together established QCD as the correct theory of the strong interactions, and made us confident that basic properties of hadron wave functions can be deduced from experimental measurements using the methods of PQCD.

The success of DIS phenomenology should not make us forget that the structure function $F_{q/N}(x, Q^2)$, no matter how completely known, still only provides a

¹This was the main topic of my talk at St. Malo. In this contribution, charm is discussed in a more detailed form, compared to the other ELFE physics issues.

very limited knowledge of the nucleon wave function. In terms of a (light-cone) Fock state expansion of the proton wave function,

$$\begin{aligned}
|p\rangle &= \int \prod_i dx_i d^2k_{\perp i} \{ \Psi_{uud}(x_i, k_{\perp i}) |uud\rangle \\
&+ \Psi_{uudg}(\dots) |uudg\rangle + \dots + \Psi_{\dots}(\dots) |uudq\bar{q}\rangle + \dots \} \quad (4)
\end{aligned}$$

the structure function $F_{q/p}$ can be expressed as a sum over the absolute squares of all Fock components n that contain a parton q with the measured momentum fraction x ,

$$F_{q/p}(x, Q^2) = \sum_n \int^{k_{\perp}^2 < Q^2} \prod_i dx_i d^2k_{\perp i} |\Psi_n(x_i, k_{\perp i})|^2 \delta(x - x_q) \quad (5)$$

Due to the average over Fock states, the most probable states will typically dominate in the structure function. Information about partons which do not participate in the hard scattering is lost in the sum of Eq. (5). The structure function is a single parton inclusive probability distribution that does not teach us about parton correlations. However, at large values of x the structure function singles out unusual Fock states where one parton carries nearly all momentum, and all other partons therefore must have low x .

2.2 Hard Exclusive Scattering

It is desirable to make measurements of hadron wave functions beyond the structure function (5). This requires special care, given that we only master the perturbative region of QCD. We need to study a hard scattering, where the subprocess can be identified and calculated, and where the dependence on the soft wave function factorizes. The factorization between hard and soft processes is a nontrivial feature in a theory like QCD with massless (long-range) gluon exchange. Even in inclusive scattering factorization has only been proved for a subset of the measurable hard processes [6].

The hard subprocess can occur coherently off several partons if the distance between them is commensurate with the momentum transfer Q . Such ('higher twist') processes are more strongly damped in momentum transfer than DIS (*cf* Eqs. (1) and (2)), since the partons must be increasingly close as Q grows. This is the case in hard exclusive processes, where factorization has also been shown to apply [7]. As an example, consider elastic electron-proton scattering, $ep \rightarrow ep$ at large momentum transfer Q (Fig. 1a). The amplitude for this process factorizes into a product of a hard scattering part T_H and proton 'distribution amplitudes' φ_p ,

$$A(ep \rightarrow ep) = \int_0^1 \prod_{i=1}^3 dx_i dy_i \varphi_p(x_i, Q^2) T_H \varphi_p(y_i, Q^2) \{1 + \mathcal{O}(1/Q^2)\} \quad (6)$$

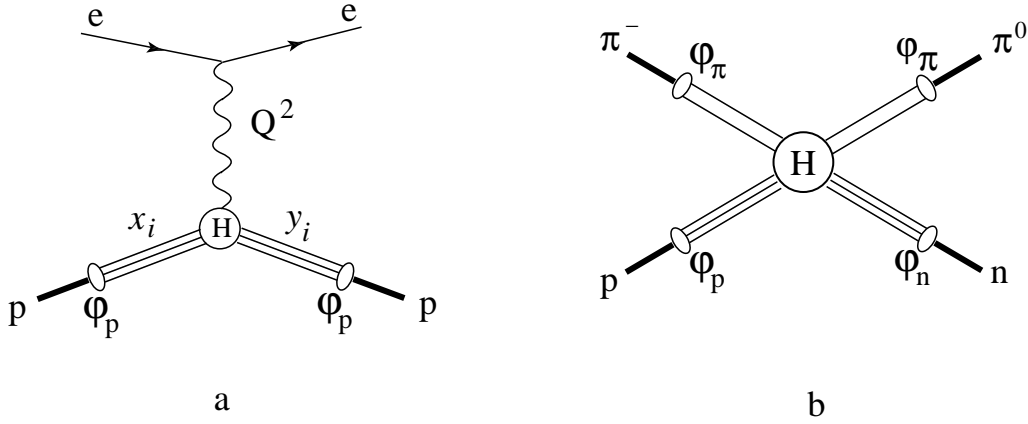


Figure 1: a. Elastic $ep \rightarrow ep$ scattering at large Q^2 factorizes into a product of proton distribution amplitudes φ_p and a hard electron scattering from the compact valence Fock state $|uud\rangle$. b. An analogous factorization is illustrated for the large angle process $\pi^- p \rightarrow \pi^0 n$.

The proton distribution amplitude is the valence part of the Fock expansion (4), integrated over relative transverse momenta up to Q ,

$$\varphi_p(x_i, Q^2) = \int^{k_{i\perp}^2 < Q^2} \prod_i d^2 \vec{k}_{i\perp} \Psi_{uud}(x_i, k_{i\perp}) \quad (7)$$

where the x_i denote the longitudinal momentum fractions of the valence uud constituents. The integral over the relative transverse momenta $k_{i\perp}$ implies that the transverse size of the valence state is $r_\perp \simeq 1/Q$. The hard amplitude T_H describes the subprocess $e + (uud) \rightarrow e + (uud)$, which selects compact $|uud\rangle$ states.

The logarithmic Q^2 dependence of the proton distribution amplitude is given by

$$\varphi_p(x_i, Q^2) = 120x_1x_2x_3\delta(1-x_1-x_2-x_3) \sum_{n=0} \left[\frac{\alpha_s(Q^2)}{\alpha_s(Q_0^2)} \right]^{\lambda_n} C_n P_n(x_i) \quad (8)$$

The anomalous dimensions form an increasing series

$$\lambda_0 = \frac{2}{27} < \lambda_1 = \frac{20}{81} < \lambda_2 = \frac{24}{81} < \dots \quad (9)$$

implying that each successive term in Eq. (8) decreases faster with Q^2 than the previous one. The P_n are Appell polynomials, $P_0 = 1$, $P_1 = x_1 - x_3$, $P_2 = 1 - 3x_2$, \dots and the C_n are constants which characterize the proton wave function and

have to be determined from experiment. The Q^2 evolution of the pion distribution amplitude is given by an expression similar to Eq. (8). The overall normalization of the pion distribution amplitude is fixed by the decay constant f_π measured in $\pi \rightarrow \mu\nu$ decay.

Just as in the case of inclusive scattering, the relevance of factorization for data on exclusive reactions must be demonstrated by showing that the same (universal) distribution amplitudes φ_h describe several hard exclusive processes. For example, large angle $\pi^- p \rightarrow \pi^0 n$ scattering should be described by the diagram of Fig. 1b, which involves the pion and proton distribution amplitudes and the $(q\bar{q}) + (qqq)$ elastic subprocess. Heavy meson decays like $B \rightarrow \pi\pi$ can also be analyzed in the same formalism (assuming that the momentum transfers involved are large enough).

Tests of factorization in exclusive reactions are quite difficult in practice. From a theoretical point of view, the calculation of multi-parton scattering amplitudes like those in Fig. 1 are very demanding even at the Born level, due to the large number of Feynman diagrams. It is also difficult to estimate how high momentum transfers are required in order to reach the scaling regime. Thus in Fig. 1a the momentum transfer Q from the electron is effectively split among the three quarks of the proton. The less momentum a quark carries, the less transfer it needs to scatter to a large angle. There is an especially dangerous region where some of the valence quarks carry a very small fraction x of the proton momentum, in which case they can fit into the proton wave function both before and after the hard scattering, without receiving any momentum transfer. There has been much discussion as to the importance of this ‘Feynman mechanism’ [8]. The consensus appears to be that it is suppressed asymptotically [7, 9] due to the Sudakov effect [10]: The single quark carrying all the momentum cannot be deflected to a large angle without gluon emission. At finite (and relevant) energies, the importance of the Feynman mechanism is still not settled – and its significance may depend on the reaction.

An immediate consequence of factorization for exclusive reactions is the ‘counting’ or ‘dimensional scaling’ rule [11], which gives the power of the squared momentum transfer t by which any $2 \rightarrow 2$ fixed angle differential cross section is suppressed (up to logarithms),

$$\frac{d\sigma}{dt}(2 \rightarrow 2) \propto \frac{f(t/s)}{t^{n-2}} \quad (10)$$

where n is the total number of elementary fields (quarks, gluons, photons) that are involved in the scattering. This rule follows from simple geometrical considerations. Elastic scattering between two elementary fields (*eg*, $qq \rightarrow qq$) involves no dimensionful quantities except s and t and thus obeys Eq. (10) with $n = 4$ at fixed t/s . Each additional field that is involved in the scattering must be within a transverse distance of order $r_\perp \lesssim 1/Q$ (with $Q^2 \simeq -t$) to scatter coherently, and the probability for that is of $\mathcal{O}(1/(Q^2 R^2))$, where $R \simeq 1$ fm is the average

radius of the hadron. This rule also explains why the dominant contribution to hard scattering comes from the valence Fock states, which minimize the power n in Eq. (10).

It is encouraging (although by no means conclusive) for factorization in hard exclusive processes that the scaling rule (10) is approximately obeyed by the data for many reactions. Thus, $ep \rightarrow ep$ involves a minimum of $n = 8$ fields, implying that the proton form factor should scale as $F_p(Q^2) \propto 1/Q^4$, as assumed in Eq. (2). Data is available [12] for $Q^2 \lesssim 30 \text{ GeV}^2$ and is consistent with this behavior for $Q^2 \gtrsim 5 \text{ GeV}^2$. At the higher values of Q^2 there are indications of scaling violations that are consistent with the logarithmic evolution predicted by Eq. (6).

Tests of the dimensional scaling rules in exclusive reactions are analogous to tests of Bjorken scaling in DIS, *ie*, that the Q^2 dependence of the inclusive cross section is given by Eq. (1). In DIS, the cross section as a function of x then directly measures the structure function $F(x)$. In exclusive reactions the situation is not as favorable. The experimentally determined normalization of the proton form factor only gives us one number, which is an average of the proton distribution amplitude integrated over the momentum fractions x_i carried by the valence quarks. To make a quantitative prediction one must know both the shape and the normalization of the (non-perturbative) distribution amplitude. The good news is that the asymptotic form of the amplitude in the $Q^2 \rightarrow \infty$ limit is known, $\varphi_p^{AS} \propto x_1 x_2 x_3$ according to Eq. (8). The non-asymptotic corrections are encoded in the moments C_i which are measurable in principle. Considerable efforts have been made to determine the pion and proton distribution amplitudes theoretically using lattice calculations and QCD sum rules [13, 14].

One of the simplest hard exclusive processes is the pion transition form factor $F_{\pi\gamma}(Q)$, measured by the process $e\gamma \rightarrow e\pi$ at large momentum transfer Q , *cf* Fig. 2a. The existing data [15] in the range $1 < Q^2 < 8 \text{ GeV}^2$ shown in Fig. 2b is well fit using a pion distribution amplitude close to the asymptotic form $\varphi_\pi^{AS} \propto x_1 x_2$ [16]. Considering that the absolute normalization in the large Q^2 limit is fixed by the pion decay constant, $F_{\pi\gamma}^{AS} = \sqrt{2} f_\pi / Q^2$, the agreement is very encouraging and indicates that the factorization formalism applies even at moderate values of Q^2 . There is evidence, on the other hand, that the asymptotic regime may be more distant in the case of the pion form factor measured by $e\pi \rightarrow e\pi$ large angle scattering [17].

There are many other processes that can and need to be analyzed experimentally and theoretically in order to achieve a comprehensive understanding of the phenomenology of hard exclusive scattering. A particularly important process is virtual compton scattering $\gamma^* p \rightarrow \gamma p$, which involves no hadrons except the proton and offers the possibility of varying independently both the virtuality of the photon and the momentum transfer to the proton [18, 19, 14, 20]. Many exclusive processes involve resonance production and thus require the measurement of multiparticle final states. It seems clear that the phenomenology of rare

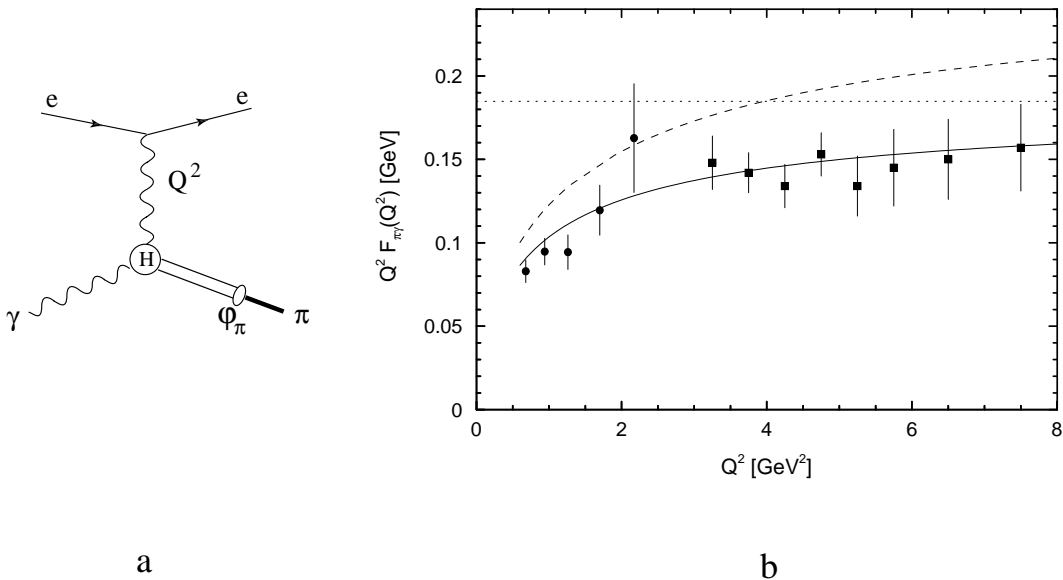


Figure 2: a. The pion transition form factor $F_{\pi\gamma}$ is measured by the process $e\gamma \rightarrow e\pi$, and factorizes at high Q^2 into a product of the calculable hard subprocess $e\gamma \rightarrow e + (q\bar{q})$ and the pion distribution amplitude φ_π . b. Data [15] compared with calculations based on a pion distribution amplitude close to the asymptotic one (solid line) and one based on QCD sum rules [13] (dashed line). The dotted line represents the asymptotic result $\sqrt{2}f_\pi$. Figure from Kroll *et al.* in [16].

exclusive processes requires the capability of an ELFE type accelerator, which combines sufficient energy with high luminosity in a continuous electron beam.

2.3 Scattering from Compact Subsystems

In inclusive DIS and in hard exclusive processes a photon (or gluon) scatters from a parton system ($q, g, q\bar{q}$ or qqq) with a transverse size of $\mathcal{O}(1/Q)$, compatible with the photon wavelength. Intuitively, this is required for the physics of the hard perturbative scattering to factorize from the non-perturbative wave function, which determines the probability for such compact systems.

Fully inclusive scattering like DIS measures single parton distributions, with no constraint on the size of the Fock state to which they belong. In exclusive scattering the whole Fock state is required to be compact. There are also hard processes where the scattering occurs off *multiparton subsystems* of the hadron, such as $qq, gg, etc.$ The theoretical framework for such processes is still incomplete, but quite recently progress has been made for meson production processes such as $\gamma^*p \rightarrow \pi^+n$ shown in Fig. 3a. In the limit where the energy ν and virtuality Q^2 of the photon are large, but the momentum transfer Δ between the nucleons remains fixed, the amplitude for this process factorizes [21] into a

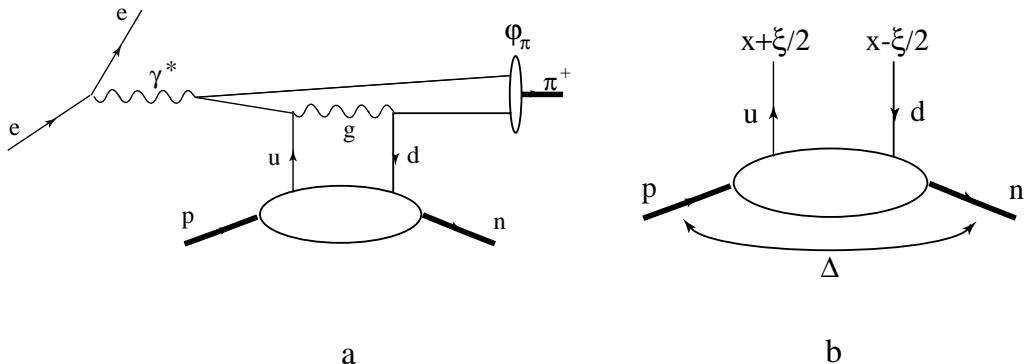


Figure 3: a. Lowest order contribution to the process $ep \rightarrow e\pi^+n$, in the limit of large ν and Q^2 but a fixed momentum transfer between the nucleons. b. An off-forward parton distribution, with the momentum fractions $x \pm \xi/2$ of the quarks and the momentum transfer Δ between the nucleons indicated.

perturbatively calculable hard subprocess (shown to lowest order in Fig. 3a), the distribution amplitude φ_π of the π^+ and an ‘Off-Forward Parton Distribution’ (OFPD) shown in Fig. 3b. As suggested by the figure, the OFPD is a generalization of the usual quark structure function measured in DIS to the non-forward ($\Delta, \xi \neq 0$) and inelastic ($p \neq n$) case.

It has been shown [14, 20, 22] that the OFPD’s interpolate between structure functions and distribution amplitudes. In the kinematic region where the light-cone momentum fractions $x \pm \xi/2$ of the quarks in Fig. 3b are both positive (or negative) the OFPD is analogous to a structure function. On the other hand, when for example $x - \xi/2 < 0$, this vertex should be regarded as the distribution amplitude of a compact $u\bar{d}$ pair in the nucleon, which carries momentum fraction ξ . In this case the physics corresponds to the virtual photon scattering off the quark pair and ejecting it from the nucleon, where it forms a π^+ . The $\gamma^*p \rightarrow \pi^+n$ process thus can give experimental information on the distribution of compact quark pairs in the nucleon.

Consider now the semi-inclusive process $ep \rightarrow e\pi + X$ sketched in Fig. 4a, where the pion takes a fraction z of the photon energy ν . In the limit $z \rightarrow 1$ the photon transfers nearly all its energy to the pion. This requirement selects compact $q\bar{q}$ configurations [23, 24]. Alternatively (and in fact equivalently), the struck quark needs to combine with a very soft antiquark to form the pion. Such asymmetric configurations are short-lived and indistinguishable (by the photon) from compact $q\bar{q}$ pairs in the limit of $z \rightarrow 1$ with fixed $(1 - z)Q^2$ [25]. Although a formal proof is still lacking, we may thus expect the cross section to factorize in this limit as

$$\sigma = F_{q\bar{q}/p}(x) \hat{\sigma}(e + (q\bar{q}) \rightarrow e + (q\bar{q})) |\varphi_\pi|^2 \quad (11)$$

where $F_{q\bar{q}/p}(x)$ is the probability for finding the compact quark pair in the target, and the pion distribution amplitude φ_π is the amplitude for the pair to transform into a physical pion.

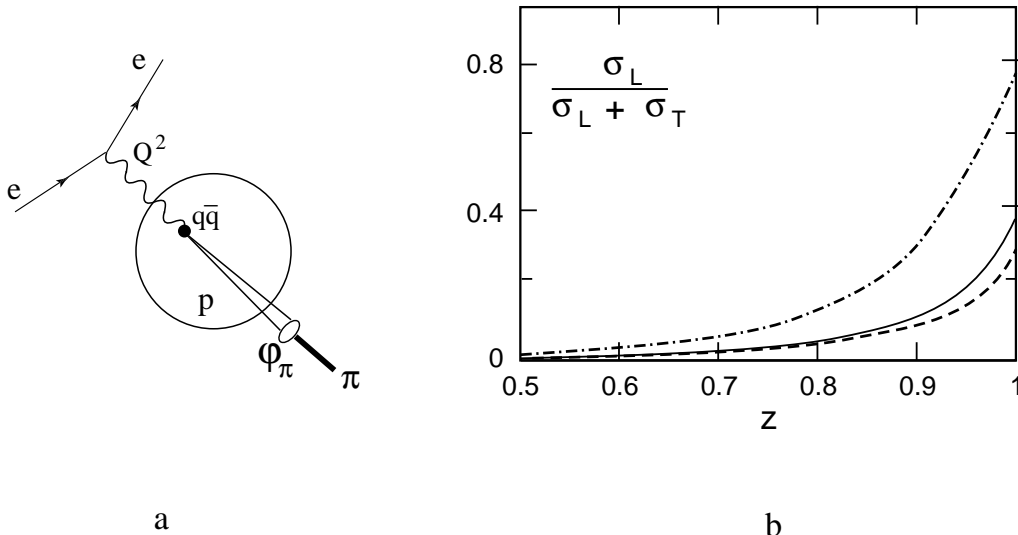


Figure 4: a. Electron scattering off compact $q\bar{q}$ pairs in the target are selected by the semi-inclusive process $ep \rightarrow e\pi + X$ when the pion carries a large fraction z of the photon energy. b. Model calculation [24] of the ratio $\sigma_L/(\sigma_L + \sigma_T)$, showing how coherent scattering on $q\bar{q}$ begins to dominate at large z . The curves correspond to different choices of the pion distribution amplitude.

Scattering off $q\bar{q}$ pairs (having integer spin) can be distinguished from scattering off single (spin 1/2) quarks through the ratio $\sigma_L/(\sigma_L + \sigma_T)$ of the longitudinally polarized to total photon cross sections. As is well known, $\sigma_L = 0$ (up to higher order QCD corrections) for scattering from spin 1/2 quarks, whereas $\sigma_T = 0$ for scattering on spin 0 diquarks. A calculation of the cross section ratio as a function of z based on the model originally proposed in Ref. [23] is shown in Fig. 4b. Experimental evidence for an analogous effect has been seen in the reverse reaction $\pi N \rightarrow \mu^+\mu^- + X$, where the muon pair takes a high fraction x_F of the pion momentum [26].

A factorization of the form (11) for semi-inclusive processes allows an interesting extension of the well-known color transparency tests [5] using proton knock-out from nuclei. In the exclusive reaction $eA \rightarrow ep(A-1)$ measured by NE-18 [27] (and in $pA \rightarrow pp(A-1)$ as measured at BNL [28]) the requirement that the final state nucleus is close to its ground state (no pion emission) selects ‘typical’ nuclear configurations. The probability to find a compact uud state is then given by the number $F_{p/A} = Z$ of protons in the nucleus multiplied

by the probability to find the uud in a free proton (see Fig. 5). The semi-inclusive reaction $eA \rightarrow epX$ with $1 - z \propto 1/Q^2$, on the other hand, can get contributions from highly excited nuclear configuration. The quarks in the compact uud state could, for example originate from separate but overlapping nucleons. Comparing proton knock-out in exclusive and semi-inclusive processes will thus tell us whether the latter contributions are significant,

$$F_{uud/A} \stackrel{?}{=} Z |\varphi_p|^2 \quad (12)$$

and hence will measure the distribution of compact multinucleon clusters in nuclei.

3 Short Range Correlations in Nuclei

The inclusive nuclear structure function is to a first approximation given by the nucleon one, $F_{q/A}(x) \simeq AF_{q/N}(x)$ [29]. Deviations of $\mathcal{O}(20 \dots 30 \%)$ are observed for small values of x ('shadowing') and for $x = 0.5 \dots 0.7$ (the 'EMC effect'). When viewed in coordinate space, one finds [30] that the quark 'mobility distribution' is almost independent (at the 2% level) of A up to light-cone distances (conjugate to $Q^2/2\nu$) of order 2 fm, with shadowing setting in at larger distances. Since DIS is dominated by the most common Fock states this indicates that typical nucleon configurations are little affected by the nuclear environment. The shadowing effect at large light-cone distances reflects coherent scattering off several nucleons in the nucleus.

In contrast to inclusive scattering, hard semi-inclusive and exclusive scattering select rare parton configurations, where some or all of the partons in the Fock state are at short relative transverse distance. Since such configurations do not contribute to DIS at moderate values of x their A -dependence is essentially unknown. Clusters that carry more momentum than single nucleons in the nucleus are of special interest, since they select nuclear configurations where several nucleons are at short relative distance. In the parlance of nuclear physics, these represent highly excited states of the nucleus (with excitation energies in the GeV region) about which we know very little at present. An electron beam of high intensity and resolution is essential for mapping out such dense clusters.

In DIS on nuclei, the fraction $x = Q^2/2m_p\nu$ of the target momentum carried by the struck quark has the range $0 \leq x \leq A$. Data at $x \gtrsim 1$ exists and is difficult to explain by standard Fermi motion [31, 32, 33]. Models based on short-range correlations between nucleons [34] and on multi-quark effects [35] can fit the data, but considerably more experimental and theoretical effort will be needed to clarify the physics of this 'cumulative' region of nuclei.

Novel cumulative effects are observed also in nuclear fragmentation into hadrons [34, 36, 37]. The hadron (p , π , K) momentum distributions extend beyond $x_F = 1$, *ie*, their momentum must have been transferred from several nucleons.

The fragmentation is only weakly dependent on the nature of the projectile or its energy, indicating that it measures features intrinsic to the nuclear wave function. In these processes the projectile scattering is soft, but there is evidence [38] that the average transverse momentum of the produced hadrons increases with x_F , reaching $\langle p_{\perp}^2 \rangle = 2 \text{ GeV}^2$ at $x_F = 4$ for protons. The cumulative momentum transfers thus appear to originate in a transversally compact region of the nucleus.

Cumulative nuclear effects have furthermore been observed in subthreshold production of antiprotons and kaons [39]. The minimal projectile energy required for the process $pp \rightarrow \bar{p} + X$ on free protons at rest is 6.6 GeV. The kinematic limit for $pA \rightarrow \bar{p} + X$ on a heavy nucleus at rest is only $3m_N \simeq 2.8 \text{ GeV}$. This reaction has been observed for $A = {}^{63}\text{Cu}$ down to $E_{lab} \simeq 3 \text{ GeV}$, very close to kinematic threshold. Scattering on a single nucleon in the nucleus would at this energy require a Fermi momentum of $\mathcal{O}(800) \text{ MeV}$. While the pA data can be fit assuming such high Fermi momenta, this assumption leads to an underestimate of subthreshold production in AA collisions by about three orders of magnitude [40].

It is possible that the subthreshold production of K and \bar{p} on nuclei involves the same compact multiparton clusters that are responsible for scattering with $x > 1$ and $x_F > 1$, although this is far from clear at present. A study of subthreshold production using lepton beams could be quite informative, since the locality of the reaction can be tuned through the virtuality of the exchanged photon. A further possibility to pin down the reaction mechanism is provided by subthreshold production of charm.

4 Charm production at ELFE

4.1 General remarks on charm(onium) production

ELFE will operate in the region of charm ($c\bar{c}$) threshold, which in the case of real photons is at $E_{\gamma}^{th} \simeq 8 \dots 12 \text{ GeV}$ for $J/\psi, \dots, D\bar{D}$ production on free nucleons. Charmonium production has proved to be a very sensitive measure of reaction mechanisms, as evidenced by order-of-magnitude discrepancies found between QCD models and data [41, 42, 43]. Furthermore, the suppression of charmonium production in heavy ion collisions is widely discussed as a potential signal for the formation of a quark-gluon plasma [44]. I shall discuss some of the puzzles of charmonium production and how photo- and electroproduction close to threshold can give important new clues to production mechanisms as well as to hadron and nuclear structure [45].

Remarkably, the only charm photoproduction data that exists (Fig. 6) in the ELFE energy range are the J/ψ measurements of SLAC [46] and Cornell [47] from 1975, which predate the discovery of open charm. These early measurements

of the small near-threshold cross section $\sigma(\gamma N \rightarrow J/\psi N) \simeq 1$ nb were made possible by the experimental cleanliness of the $J/\psi \rightarrow \mu\mu$ signal. With an ELFE luminosity $\mathcal{L} \sim 10^{35} \text{cm}^{-2}\text{s}^{-1}$ one expects a rate of about 5 J/ψ dimuon decays per second, allowing detailed measurements of threshold and subthreshold effects.

It should also be kept in mind that owing to the essentially non-relativistic nature of charmonium, each charm quark carries close to one half of the J/ψ momentum. Even their relative angular momentum is determined through the quantum numbers of the charmonium state. Charmonium is thus a very valuable complement to open charm channels such as $D\bar{D}$, which furthermore are difficult to measure.

Theoretically, charmonium offers very interesting challenges. Most reliable QCD tests have so far concerned hard inclusive scattering, implying a sum over a large number of open channels. The standard QCD factorization theorem [6] does not apply when the final state is restricted by requiring the charm quarks to bind as charmonium. The application of QCD to charmonium production is thus partly an art, as evidenced by lively discussions of different approaches. It seems likely that charmonium production will teach us something qualitatively new about QCD effects in hard scattering – exactly what is not yet clear (but hopefully will be so by the time ELFE turns on!).

4.2 J/ψ production at high energies

4.2.1 Elastic J/ψ Production

Early studies [48] assumed that the charmonium cross section is proportional to the $c\bar{c}$ one below open charm ($D\bar{D}$) threshold, as given by the inclusive photon-gluon fusion process $\gamma g \rightarrow c\bar{c}$. Thus

$$\sigma(\gamma N \rightarrow J/\psi + X) = f_{J/\psi} \int_{4m_c^2}^{4m_D^2} \frac{dM^2}{s} G(M^2/s) \sigma_{\gamma g \rightarrow c\bar{c}}(M^2) \quad (13)$$

where $G(x)$ is the gluon structure function and the proportionality constant $f_{J/\psi}$ is the fraction of the below-threshold $c\bar{c}$ pairs that form J/ψ 's. In this ‘Color Evaporation Model’ (CEM) the color exchanges which transform the color octet $c\bar{c}$ pair into a color singlet J/ψ are assumed to occur over long time and distance scales, and are described by the non-perturbative factor $f_{J/\psi}$ in Eq. (13). For the model to have predictability it is important that this factor be ‘universal’, *ie*, independent of the reaction kinematics (beam energy and charmonium momentum), and hopefully also of the nature of the projectile and target. It should be emphasized, however, that the universality of $f_{J/\psi}$ is a hypothesis which has not been demonstrated in QCD.

Assuming a constant $f_{J/\psi}$ and a ‘standard’ gluon structure function $xG(x) = 3(1-x)^5$, Eq. (13) (with $X = N$) gives a good fit (solid line in Fig. 6) to J/ψ elastic photoproduction from threshold to $E_\gamma \lesssim 300$ GeV [49]. It is not very clear

what this means, however. Close to threshold the single gluon exchange picture is expected to break down (*cf* section 4.3.1). At high energy, color evaporation is expected to apply to *inelastic* processes, since the neutralization of color will lead to additional hadrons being produced.

A consistent QCD description of high energy elastic J/ψ photoproduction involves two gluon (color singlet) exchange between the charm quark pair and the target [50]. In this approach the color dynamics of the charm quark pair is treated perturbatively, *ie*, the quarks are created as a compact color singlet state which couples directly to the J/ψ through the wave function at the origin. This is justified by the factorization between the hard and soft physics in this process [21]. As discussed in Sect. 2.3 the two gluon coupling to the target is an off-forward gluon distribution which near the forward direction may be similar to the gluon structure function measured by deep inelastic scattering [22]. The elastic J/ψ cross section may thus be approximately proportional to the *square* of the gluon structure function. The high energy data (Fig. 7) on $\gamma p \rightarrow J/\psi p$ from HERA [51, 52] in fact shows a considerable rise of the elastic cross section with energy, which (within the considerable error bars) is consistent with the increase of $xG(x)$ for $x \simeq 4m_c^2/s \rightarrow 0$ [53].

4.2.2 Color Evaporation Approach to Inelastic J/ψ Production

The difficulties of perturbative QCD models in describing the data on inelastic charmonium production (*cf* sections 2.3 and 2.4 below) has rekindled interest in the color evaporation model [54, 55, 56, 57]. It has been shown that the dependence of both charmonium and bottomonium production on the projectile energy and on the energy fraction x_F of the produced state are in good agreement with that predicted through Eq. (13) for heavy quarks below threshold. The fraction of the below-threshold heavy quark cross section which ends up in quarkonium depends on the QCD parametrization (quark mass, structure functions and factorization scale) but seems to be quite small, typically (8 ... 10)% for charm, growing to (17 ... 32)% for bottom [57]. The parameter $f_{J/\psi}$ of Eq. (13) takes similar values in pp and πp reactions (0.025 and 0.034, respectively [54]). In photoproduction the large diffractive (elastic) peak needs to be excluded, *eg*, by a cut on the J/ψ momentum, after which values in the range $f_{J/\psi} = 0.005 \dots 0.025$ were found [57].

The generally good agreement of the color evaporation model with data is very significant. It shows that the essential structure of the inclusive charmonium cross section is given by that of heavy quark production at leading twist. According to the spirit of color evaporation, the heavy quarks will after their production undergo a long time-scale process of evolution to the quarkonium bound state, during which the relative distance between the quarks grows and non-perturbative gluons change the overall color of the quark pair. The normalization of the production cross section, *ie*, the non-perturbative parameter $f_{J/\psi}$ in Eq. (13), is

thus not necessarily related to the wave function at the origin of the charmonium bound state.

4.2.3 The Color Singlet Model (CSM)

The ‘Color Singlet Model’ (CSM) [58] describes charmonium production fully in terms of PQCD. The $c\bar{c}$ is created with proper quantum numbers to have an overlap with the charmonium state, measured by the non-relativistic wave function at the origin. In particular, the pair has to be a singlet of color. For inelastic J/ψ photoproduction the lowest order subprocess is $\gamma g \rightarrow c\bar{c}g$, where the final gluon radiation ensures that the charmonium is produced with an energy fraction (in the target rest frame) $z = E_{J/\psi}/E_\gamma < 1$. For production at large $p_\perp \gg m_c$ higher order ‘fragmentation diagrams’ actually give the leading contribution [59].

The CSM contributions to J/ψ photoproduction have been calculated to next-to-leading order in QCD [60], with a result that is in good agreement with the data (Fig. 8). For ψ' production the CSM predicts that the ψ'/ψ cross section ratio should be proportional to the square of the wave function at the origin,

$$\frac{\sigma(\psi')}{\sigma_{dir}(J/\psi)} = \frac{\Gamma(\psi' \rightarrow \mu\mu)}{M_{\psi'}^3} \frac{M_{J/\psi}^3}{\Gamma(J/\psi \rightarrow \mu\mu)} \simeq .24 \pm .03 \quad (14)$$

Here $\sigma_{dir}(J/\psi)$ excludes contributions to the J/ψ from ‘indirect’ channels such as B , χ_c and ψ' decays, and the power of mass is motivated by dimensional arguments. The photoproduction data [62, 63] gives for the ratio that is uncorrected for radiative decays,

$$\frac{\sigma(\gamma N \rightarrow \psi' + X)}{\sigma(\gamma N \rightarrow J/\psi + X)} = 0.20 \pm 0.05 \pm 0.07 \quad (15)$$

The upper limit on the $\chi_{c1} + \chi_{c2}$ photoproduction cross section is about 40% of the J/ψ cross section [62]. Taking into account the $\mathcal{O}(20\%)$ branching ratio for their radiative decays into J/ψ only a small fraction of the photoproduced J/ψ 's are due to the indirect channels, and the ratios of Eqs. (14) and (15) should be compatible, as indeed they are. It should be noted, however, that the experimental ratio (15) primarily reflects diffractive (elastic) J/ψ and ψ' production, which dominates in photoproduction.

In hadroproduction, where inelastic channels dominate the cross section, data on the ratio (14) is also in good agreement with the color singlet model [64]. This is true as well for the Tevatron data on charmonium production at large p_\perp [42]. Even bottomonium production is quite consistent with the analog of Eq. (14), within factor of two uncertainties due to the so far unmeasured contributions from radiative decays of the P states [54].

The above comparisons suggest that the ‘nonperturbative’ proportionality factors f in the color evaporation model (*cf* Eq. (13)) actually reflect perturbative physics, *ie*, the wave function at the origin as assumed in the color singlet model.

In spite of its successful predictions in photoproduction and of the *ratio* of ψ' to J/ψ hadroproduction, the CSM nevertheless fails badly, by factors up to 30 ... 50, for the *absolute hadroproduction* cross sections of the J/ψ , the ψ' and the χ_{c1} states [41, 42, 43, 64]. The discrepancies are large both in fixed target total cross section data and in large p_{\perp} production at the Tevatron. The fixed target data moreover shows that the J/ψ and ψ' are produced nearly unpolarized [65], contrary to the CSM which predicts a fairly large transverse polarization [64].

The fact that the CSM *underestimates* charmonium hadroproduction (and predicts the polarization incorrectly), suggests that there are other important production mechanisms, beyond the CSM. The nature of those processes is not yet established. A simple mnemonic, which appears to be consistent with the observed systematics, is that the CSM works whenever no extra gluon emission is required only to satisfy the quantum number constraints. Thus, for inelastic J/ψ photoproduction the lowest order process $\gamma g \rightarrow c\bar{c}g$ of the CSM has only the number of gluons which is required by momentum transfer (and the prediction is successful). In the (incorrect) CSM prediction for hadroproduction gluon emission in the subprocess $gg \rightarrow c\bar{c}g$ is needed only due to the negative charge conjugation of the J/ψ (or due to Yang’s theorem in the case of χ_{c1} production). Again, for χ_{c2} the lowest order process $gg \rightarrow \chi_{c2}$ is allowed in the CSM, and the prediction is compatible with the data (within the considerable PQCD uncertainties) [43, 64, 66]. A polarization measurement of hadroproduced χ_{c2} ’s would be a valuable check of the CSM [64, 67].

Photoproduction of χ_c is an interesting test case [57, 61]. The available data [62] suggests that the $\chi_{c2}/J/\psi$ ratio is lower in inelastic photoproduction than in hadroproduction. This qualitatively agrees with the CSM, in which P -wave photoproduction ($\gamma g \rightarrow \chi_{c2}gg$) is of higher order than S -wave production ($\gamma g \rightarrow J/\psi g$), while the reverse is true for hadroproduction. With no regard to quantum numbers (as in the color evaporation model) the basic subprocess would be the same ($\gamma g \rightarrow c\bar{c}$) and the $\chi_c/J/\psi$ ratio would be expected to be similar in photo- and hadroproduction.

It has been suggested that the gluons required to satisfy quantum number constraints of the $c\bar{c}$ pair in the CSM could come from additional (higher twist) exchanges with the projectile or target [64, 68]. Although normally suppressed, these contributions might be important since they do not involve energy loss through gluon emission.

4.2.4 The Color Octet Model (COM)

A possible solution to some of the above puzzles has been suggested based on an analysis of nonrelativistic QCD (NRQCD) [69], and commonly referred to as the

‘Color Octet Model’ (COM) [66, 70]. In cases where, due to quantum number constraints, extra gluon emission is required in the CSM the production may be dominated instead by higher order terms in the relativistic (v/c) expansion of the quarkonium bound state. For P -wave states the inclusion of relativistic corrections is in fact necessary to cancel infrared divergencies of the perturbative expansion even at lowest order.

The $c\bar{c}$ can then be produced in a color octet state, which has an overlap with a higher $|c\bar{c}g\rangle$ Fock state of charmonium, with the emission of a soft gluon. Such contributions appear in a systematic NRQCD expansion and thus must exist. Whether they are big enough to account for the large discrepancies of the CSM in charmonium production depends on the magnitude of certain non-perturbative matrix elements of NRQCD. I refer to recent reviews [43, 71] and references therein to the extensive literature on this subject.

A number of discrepancies between the color octet model and observations suggest that it will at best provide only a partial explanation of quarkonium production.

- (i) Inelastic photoproduction of J/ψ is overestimated by the COM [61, 72] as seen in Fig. 8. A best estimate of the discrepancy is actually even larger than shown, since the effects of soft gluon radiation were neglected in fitting the octet matrix elements from the Tevatron data [73]. The photoproduction cross section can be *decreased* in the COM only by adding a contribution which is coherent with the production amplitude.
- (ii) The COM does not explain the p_\perp -integrated (fixed target) charmonium hadroproduction data, in particular not the polarization of the J/ψ and ψ' and the χ_{c1}/χ_{c2} ratio [74, 75, 76]. It has been claimed, but is by no means obvious, that the (higher twist?) corrections are bigger in the fixed target data than in the large p_\perp cross section measured at the Tevatron, which is often taken as a benchmark for COM fits. The systematics of the anomalies is actually very similar in the two processes. The color singlet model fails by a comparable factor in both cases [42], while the (leading twist) color evaporation model successfully explains the relative production rates measured in the fixed target and Tevatron experiments [56, 57].
- (iii) The $\Upsilon(3S)$ cross section exceeds the CSM predictions by an order of magnitude [42, 77]. Since the relativistic corrections are much smaller for bottomonium than for charmonium, this is hard to accommodate in the COM [75]. It has been suggested that the excess could be due to radiative decay from a hitherto undiscovered $3P$ state. As in the case of the ‘ ψ' anomaly’, an experimental measurement of direct Υ production should settle this question. The ratios of $\Upsilon(nS)$ cross sections are quite compatible with expectations based on the wave function at the origin (*cf* Eq. (14)), with only moderate contributions from radiative decays of P states [54].

4.2.5 Nuclear Target A -Dependence

Additional clues to quarkonium production dynamics is offered by data on the nuclear target A -dependence [78]. In the standard parametrization

$$\sigma(A) \propto A^\alpha \quad (16)$$

one expects $\alpha \simeq 1$ for hard incoherent scattering, which is additive on all nucleons in the target nucleus. This behavior is verified with good precision for the Drell-Yan process of large-mass lepton pair production [79] as well as for open charm (D meson) production at low x_F [80]. However, for J/ψ and ψ' hadroproduction $\alpha \simeq 0.92 \pm .01$ for $.1 \lesssim x_F \lesssim .3$ [81]. This suppression may be interpreted as a rescattering of the charm quark pair in the nucleus, with an effective cross section of 7 mb [44] for conversion to open charm production. Such rescattering will affect the quantum numbers of the $c\bar{c}$ pair, and should thus be considered in color singlet and octet approaches. For the color evaporation model the target dependence shows that the proportionality factor $f_{J/\psi}$ in Eq. (13) is not universal for all processes.

The nuclear suppression of J/ψ and ψ' production increases with x_F , with $\alpha(x_F = .6) \simeq .8$ [81]. This effect, which breaks leading twist factorization [82], may be due to intrinsic charm [83, 84] and involve the scattering of low momentum valence quarks [25]. Ascribing the effect to parton energy loss in the nucleus requires the $\langle p_\perp \rangle$ in the rescattering to be unexpectedly large [85, 86]. The dynamics of charmonium production at large x_F is analogous to the large p_\perp Tevatron data due to the ‘trigger bias’ effect: In both cases the charmonium carries a large fraction of the momentum of the fragmenting particle.

In inelastic (virtual) photoproduction a nuclear *enhancement* of J/ψ production is observed, $\alpha = 1.05 \pm 0.03$ for $x_F < 0.85$ and $p_\perp^2 > 0.4 \text{ GeV}^2$ [63, 87]. Contrary to hadroproduction, the momentum distribution of J/ψ photoproduction peaks at large x_F . Hence an explanation in terms of energy loss is conceivable [88].

In the region of the coherent peak for J/ψ photoproduction on nuclei at very low p_\perp there is an even stronger nuclear enhancement. E691 [87] finds $\alpha_{coh} = 1.40 \pm 0.06 \pm 0.04$, while NMC [63] gives $\alpha_{coh} = 1.19 \pm 0.02$. If the $c\bar{c}$ pairs are compact enough not to suffer secondary interactions in the nucleus, one expects $d\sigma_{coh}/dp_\perp^2 \propto A^2 \exp(-cA^{2/3}p_\perp^2)$ (c being a constant). Hence $\alpha_{coh} = 4/3$ for the p_\perp -integrated cross section, in rough agreement with the data.

As should be clear from the above, quarkonium production offers interesting challenges, which are not fully met by any one proposed mechanism. It seems likely that we are learning something about color dynamics that cannot be accessed within the standard, fully inclusive formalism of PQCD. Color exchanges to the $c\bar{c}$ evidently take place in ways not adequately described by the CSM. The importance of the NRQCD contributions (which surely are present at some

level) remains to be clarified, as does the assumption by the color evaporation approach that charmonium production constitutes a universal fraction of the $c\bar{c}$ cross section below open charm threshold.

4.3 Production Near Kinematic Threshold

As noted in Sect. 4.1, almost all experimental information on charmonium production is at relatively high energy. While we may hope that at least some of the puzzles discussed in the preceding section will be solved in the near future, an understanding of production near threshold will have to wait for a dedicated machine like ELFE. In the following I shall discuss some generic features of (sub-)threshold charmonium production related to the composite nature of the beam and/or target² [45]. It is likely that charm production close to threshold will teach us new physics, over and beyond what is now being learnt at higher energies.

4.3.1 Higher Twist Effects

At high energy the dominant contribution to hard processes comes from ‘leading twist’ diagrams, characterized by only one parton from each colliding particle participating in the large momentum transfer (Q) subprocess. Since the time scale of the hard collision is $1/Q$, only partons within this transverse distance can affect the process. The likelihood that two partons are found so close to each other is typically proportional to the transvers area $1/Q^2$, which thus gives the suppression of higher twist, multiparton contributions.

Close to the kinematic boundary the higher twist effects are enhanced, however. Thus for $\gamma p \rightarrow c\bar{c}p$ very near threshold, all the partons of the proton have to transfer their energy to the charm quarks within their creation time $1/m_c$, and must thus be within this transverse distance from the $c\bar{c}$ and from each other. The longitudinal momentum transfer at threshold (in the proton rest frame) is $\simeq m_c$. Hence only compact proton Fock states, with a radius equal to the compton wavelength of the heavy quark, can contribute to charm production at threshold.

The behavior of the effective proton radius in charm photoproduction near threshold can be surmised from the following argument. As indicated in Fig. 9a, one mechanism for charm production is that most of the proton momentum is first transferred to one (valence) quark, followed by a hard subprocess $\gamma q \rightarrow c\bar{c}q$. If the photon energy is $E_\gamma = \zeta E_\gamma^{th}$, where E_γ^{th} is the energy at kinematic threshold ($\zeta \gtrsim 1$), the valence quark must carry a fraction $x = 1/\zeta$ of the proton’s (light-cone) momentum. The lifetime of such a Fock state (in a light-cone or infinite

² Calculations of higher order perturbative, leading twist effects in heavy quark production near threshold may be found in Ref. [89].

momentum frame) is $\tau \simeq 1/\Delta E$, where

$$\Delta E = \frac{1}{2p} \left[m_p^2 - \sum_i \frac{p_{i\perp}^2 + m_i^2}{x_i} \right] \simeq -\frac{\Lambda_{QCD}^2}{2p(1-x)} \quad (17)$$

For $x = 1/\zeta$ close to unity such a short-lived fluctuation can be created (as indicated in Fig. 9a) through momentum transfers from valence proton states (where the momentum is divided evenly) having commensurate lifetimes τ , *ie*, with

$$r_{\perp}^2 \simeq \frac{1}{p_{\perp}^2} \simeq \frac{\zeta - 1}{\Lambda_{QCD}^2} \quad (18)$$

This effective proton size thus decreases towards threshold ($\zeta \rightarrow 1$), reaching $r_{\perp} \simeq 1/m_c$ at threshold, $\zeta - 1 \simeq \Lambda_{QCD}^2/m_c^2$.

As the lifetimes of the contributing proton Fock states approach the time scale of the $c\bar{c}$ creation process, the time ordering of the gluon exchanges implied by Fig. 9a ceases to dominate higher twist contributions such as that of Fig. 9b [25], which are related to intrinsic charm [83]. There are in fact reasons to expect that the latter diagrams give a dominant contribution to charmonium production near threshold. First, there are many more such diagrams. Second, they allow the final state proton to have a small transverse momentum (the gluons need $p_{\perp} \simeq m_c$ to couple effectively to the $c\bar{c}$ pair, yet the overall transfer can still be small in Fig. 9b). Third, with several gluons coupling to the charm quark pair its quantum numbers can match those of a given charmonium state without extra gluon emission.

The above discussion is generic, and does not indicate how close to threshold the new effects actually manifest themselves. While more quantitative model calculations certainly are called for, this question can only be settled by experiment. It will be desirable to measure both the cross section and polarization for several charmonium states, as well as for open charm. At present, there are only tantalizing indications for novel phenomena at charm threshold, namely:

- *Fast $c\bar{c}$ pairs in the nucleon.* The distribution of charm quarks in the nucleon, as measured by deep inelastic lepton scattering, appears [90] to be anomalously large at high x , indicating a higher twist intrinsic charm component [83]. An analogous effect is suggested by the high x_F values observed in $\pi N \rightarrow J/\psi + J/\psi + X$ [91]. A proton Fock state containing charm quarks with a large fraction of the momentum will enhance charm production close to threshold.
- *J/ψ polarization in $\pi^- p \rightarrow J/\psi + X$ for $x_F \rightarrow 1$.* Only compact projectile (π) Fock states contribute in the limit where the J/ψ carries almost all of the projectile momentum. It may then be expected that the helicity of the J/ψ equals the helicity of the projectile, *ie*, the J/ψ should be longitudinally polarized. This effect is observed both in the above reaction [65] and (as already discussed in Sect. 2.3) in $\pi N \rightarrow \mu^+ \mu^- + X$ [26].

- *Polarization in $pp \rightarrow pp$ large angle scattering.* There is a sudden change in the A_{NN} polarization parameter close to charm threshold for 90° scattering [92]. It has been suggested that this is due to an intermediate state containing a $c\bar{c}$ pair, which has low angular momentum due to the small relative momenta of its constituents [93]. This idea could be tested at ELFE by investigating correlations between polarization effects in large angle compton scattering, $\gamma p \rightarrow \gamma p$, and charm production ($\gamma p \rightarrow c\bar{c}p$) near threshold.
- *Change in color transparency at charm threshold.* Intermediate states with a charm quark pair could also give rise to the sudden decrease in color transparency observed in $pA \rightarrow pp(A-1)$ close to charm threshold [28]. Due to the low momentum of the constituents they expand to a large transverse size within the nucleus, thus destroying transparency [93]. Again, eA reactions could provide important tests at ELFE.

4.3.2 Subthreshold production

The high luminosities at ELFE will allow detailed studies of subthreshold production of charm(onium). It is well established that antiprotons and kaons are produced on nuclear targets at substantially lower energies than is kinematically possible on free nucleons [39]. Thus the minimal projectile energy required for the process $pp \rightarrow \bar{p} + X$ on free protons at rest is 6.6 GeV, while the kinematic limit for $pA \rightarrow \bar{p} + X$ on a heavy nucleus at rest is only $3m_N \simeq 2.8$ GeV. Antiproton production has been observed in $p + {}^{63}\text{Cu}$ collisions down to $E_{lab}^p \simeq 3$ GeV, very close to kinematic threshold. Scattering on a single nucleon in the nucleus would at this energy require a fermi momentum of $\mathcal{O}(800)$ MeV. While the pA data can be fit assuming such high Fermi momenta, this assumption leads to an underestimate of subthreshold production in AA collisions by about three orders of magnitude [40].

There are at least two qualitatively different scenarios for the observed subthreshold production of antiprotons. Either (Fig. 10a) the projectile strikes a local ‘hot spot’ with a high energy density in the nucleus. The effective mass of the scatterer is high, lowering the kinematic threshold. Alternatively (Fig. 10b) the momentum required to create the antiproton is not transferred locally, but picked up in an extended longitudinal region: the nucleus forms a ‘femtoaccelerator’. Establishing either scenario would teach us something qualitatively new about rare, highly excited modes of the nucleus.

Real and virtual photoproduction of charm below threshold would be of crucial help in distinguishing the correct reaction mechanism, for several reasons.

- The photon is pointlike, and is thus a clean probe of target substructure. In particular, effects due to the shrinking effective size of a hadron probe near threshold (*cf* discussion above) are eliminated.

- The $c\bar{c}$ pair is created locally, within a proper time $\tau \simeq 1/m_c$. The extended acceleration scenario of Fig. 10b is thus not effective for charm production. If significant subthreshold charm production occurs (beyond what can be ascribed to standard fermi motion) this selects the hot spot scenario of Fig. 10a.
- Subthreshold production can be studied as a function of the virtuality Q^2 of the photon. Little Q^2 dependence is expected for $Q^2 \lesssim m_c^2$, due to the local nature of charm production. Nuclear hot spots smaller than $1/m_c$ would be selected at higher values of Q^2 .

4.3.3 Interactions of $c\bar{c}$ Pairs in Nuclei

Close to threshold for the process $\gamma p \rightarrow J/\psi p$ on stationary protons the energy of the J/ψ is $E_{J/\psi}^{lab} \simeq 7$ GeV. This corresponds to a moderate lorentz γ -factor $E_{J/\psi}/M_{J/\psi} \simeq 2.3$. Hence a significant expansion of the $c\bar{c}$ pair occurs inside large nuclei, and effects of charmonium bound states in nuclei may be explored.

Compared to the propagation of light quarks in nuclei, charm has the advantage that one can readily distinguish hidden (charmonium) from open ($D\bar{D}$) charm production. Thus the dependence of the $\sigma(J/\psi)/\sigma(D)$ ratio on the target size A and on projectile energy indicates the amount of rescattering in the nucleus. The presently available data on the A -dependence of charmonium production is at much higher energies (*cf* Sect. 4.2.5), and thus measures the nuclear interactions of a compact $c\bar{c}$ pair rather than of full-sized charmonium. Further information about the significance of the radius of the charmonium state can be obtained by comparing ψ' to J/ψ production on various nuclei. In high energy hA and γA scattering both states have very similar A -dependence [81].

Information about the propagation of charmonium in nuclei is very important also for relativistic heavy ion collisions, where charmonium production may be a signal for quark-gluon plasma formation [44]. Precise information from ELFE would allow a more reliable determination of the background signal from charmonium propagation in ordinary nuclear matter.

Even though the $c\bar{c}$ pair is created with rather high momentum even at threshold, it may be possible to observe reactions where the pair is captured by the target nucleus, forming ‘nuclear-bound quarkonium’ [94]. This process should be enhanced in subthreshold reactions. There is no Pauli blocking for charm quarks in nuclei, and it has been estimated there is a large attractive van der waals potential binding the pair to the nucleus [95]. The discovery of such qualitatively new bound states of matter would be a scoop for any accelerator.

5 Conclusions

There are (at least) three central physics areas which require an accelerator with the capabilities of ELFE as given in Table 1:

- The determination of hadron and nuclear wave functions.
- Specifically nuclear effects: Color transparency [5], cumulative phenomena [31] – [40].
- Charm(onium) production near threshold.

In addition to these core topics there are a number of areas where ELFE can improve on presently available data, such as

- The nucleon structure function for $0.7 \lesssim x \lesssim 1$,
- Higher twist corrections of the form $c(x)/Q^2$,
- $R = \sigma_L/\sigma_T$,
- The gluon structure function,
- Polarized structure functions.

Significant advances in these areas are, however, expected from other experiments before ELFE starts operating.

Finally, we should keep in mind that the whole area of ‘confinement’ physics is very important but at present poorly understood in QCD. It includes open questions like the influence of the QCD vacuum on scattering processes [96] and the foundations of the non-relativistic quark model (see, *eg*, [97, 98]). It is difficult to assess today what the progress will be in this field. Nevertheless, it seems clear that systematic measurements of non-perturbative wave functions as discussed above will form an essential part of any serious effort to understand the hadron spectrum.

Acknowledgements. I am grateful to the organizers of this meeting for their invitation to discuss physics in a stimulating atmosphere and a delightful setting. I also wish to thank S. Brodsky and M. Vänttinen, in particular, for longstanding collaborations on the issues presented above, as well as B. Kopeliovich and M. Strikman for several useful discussions.

References

- [1] B. H. Wiik, *Future Electron Accelerators and Free Electron Lasers*, Talk at the meeting on Future Accelerators and Free Electron Lasers, Uppsala, 25-26 April 1996.

- [2] B. Frois, Talk at the meeting on Future Accelerators and Free Electron Lasers, Uppsala, 25-26 April 1996; A. Tkatchenko, Talk at the Second ELFE Workshop, St. Malo, 22-27 September 1996.
- [3] B. Frois and B. Pire, Invited talk at 8th International Nuclear Physics Conference (INPC 95), Beijing, P.R. China, 21-26 Aug 1995, hep-ph/9512221; J. Arvieux and B. Pire, Prog. Part. Nucl. Phys. **35** (1995) 299.
- [4] S. J. Brodsky, Talk presented at Orbis Scientiae (Miami Beach 1996), SLAC-PUB-7152, hep-ph/9604391.
- [5] N. N. Nikolaev and B. G. Zakharov, Talk at the INPC Conference, Beijing, China, August 1995, KFA-IKP(TH)-1995-21, nucl-th/9509036; P. Hoyer, Talk at Workshop on Deep Inelastic Scattering and QCD (DIS 95), Paris, France, April 1995, proceedings Paris DIS 1995:127, hep-ph/9510394.
- [6] J. C. Collins, D. E. Soper and G. Sterman, in *Perturbative QCD*, ed. A.H. Mueller (World Scientific, 1989); G. Bodwin, Phys. Rev. **D31** (1985) 2616 and **D34** (1986) 3932 (E); J. Qiu and G. Sterman, Nucl. Phys. **B353** (1991) 105 and **B353** (1991) 137.
- [7] For a review, see S. J. Brodsky and G. P. Lepage in *Perturbative QCD*, edited by A. H. Mueller (World Scientific, Singapore, 1989).
- [8] N. Isgur and C. H. Llewellyn-Smith, Nucl. Phys. **B317** (1989) 526; A. V. Radyushkin, Nucl. Phys. **A532** (1991) 141c.
- [9] J. Botts and G. Sterman, Nucl. Phys. **B325** (1989) 62.
- [10] V. V. Sudakov, Sov. Phys. JETP **3** (1956) 65.
- [11] S. J. Brodsky and G. R. Farrar, Phys. Rev. Lett. **31** (1973) 1153; V. A. Matveev, R. M. Muradyan and A. V. Tavkhelidze, Lett. Nuovo Cimento **7** (1973) 719.
- [12] A. F. Sill *et al.*, Phys. Rev. **D28** (1993) 860.
- [13] V. L. Chernyak and A. R. Zhitnitsky, Phys. Rep. **112** (1984) 173; S. V. Mikhailov and A. V. Radyushkin, Phys. Rev. **D45** (1992) 1754; A. V. Radyushkin and R. Ruskov, Phys. Lett. **B374** (1996) 173.
- [14] A. V. Radyushkin, Talk at Workshop on Virtual Compton Scattering, Clermont-Ferrand, France, June 1996, JLAB-THY-96-06, hep-ph/9609387.
- [15] CELLO Collaboration, H.-J. Behrend *et al.*, Z. Phys. **C49** (1991) 401; CLEO Collaboration, V. Savinov *et al.*, proceedings of the PHOTON '95 Workshop Sheffield, England, April 1995, hep-ex/9507005.

- [16] A. V. Radyushkin and R. Ruskov, CEBAF-TH-95-18, hep-ph/9603408; P. Kroll and M. Raulfs, Phys. Lett. **B387** (1996) 848, hep-ph/9605264.
- [17] R. Jakob and P. Kroll, Phys. Lett. **B315** (1993) 463; **B319** (1993) 545 (E).
- [18] M. A. Shupe *et al.*, Phys. Rev. **D19** (1979) 1929.
- [19] A. S. Kronfeld and B. Nižić, Phys. Rev. **D44** (1991) 3445; G. R. Farrar, K. Huleihel and H. Zhang, Nucl. Phys. **B349** (1991) 655.
- [20] X. Ji, MIT-CTP-2568, hep-ph/9609381.
- [21] J. C. Collins, L. Frankfurt and M. Strikman, CERN-TH-96-314, hep-ph/9611433.
- [22] X. Ji, MIT-CTP-2517, hep-ph/9603249; A.V. Radyushkin, Phys. Lett. **B385** (1996) 333, hep-ph/9605431.
- [23] E. L. Berger and S. J. Brodsky, Phys. Rev. Lett. **42** (1979) 940; A. Brandenburg, S. J. Brodsky V. V. Khoze and D. Muller, Phys. Rev. Lett. **73** (1994) 939, hep-ph/9403361; K. J. Eskola, P. Hoyer, M. Vanttinen and R. Vogt, Phys. Lett. **B333** (1994) 526, hep-ph/9404322.
- [24] A. Brandenburg, V. V. Khoze and D. Muller, Phys. Lett. **B347** (1995) 413, hep-ph/9410327.
- [25] S. J. Brodsky, P. Hoyer, A. H. Mueller and W.-K. Tang, Nucl. Phys. **B369** (1992) 519.
- [26] E615 Collaboration, J. S. Conway *et al.*, Phys. Rev. **D39** (1989) 92.
- [27] NE-18 Collaboration, N. C. R. Makins *et al.*, Phys. Rev. Lett. **72** (1994) 1986; T. G. O'Neill *et al.*, Phys. Lett. **B351** (1995) 87.
- [28] R. S. Carroll *et al.*, Phys. Rev. Lett. **61** (1988) 1698.
- [29] M. Arneodo, Phys. Rep. **240** (1994) 301.
- [30] P. Hoyer and M. Vanttinen, NORDITA-96-20-P, hep-ph/9604305.
- [31] BCDMS Collaboration, A. C. Benvenuti *et al.*, Z. Phys. **C63** (1994) 29.
- [32] J. Arrington *et al.*, Phys. Rev. **C53** (1996) 2248.
- [33] CCFR/NuTeV Collaboration, M. Vakili *et al.*, in *Proceedings of the Division of Particles and Fields meeting, 1996 (DPF96)*, Minneapolis, USA, August, 1996.

- [34] L. L. Frankfurt and M. Strikman, Phys. Rep. **160** (1988) 235; L. L. Frankfurt, M. I. Strikman, D. B. Day and M. Sargsyan, Phys. Rev. **C48** (1993) 2451.
- [35] A. V. Efremov, Sov. J. Part. Nucl. **13** (1982) 254; L. Kaptari and A. Umnikov, JINR Rapid Commun. **32** (1988) 17; S. Gupta and R. M. Godbole, Phys. Lett. **228B** (1989) 129.
- [36] V. S. Stavinskii, Sov. J. Part. Nucl. **10** (1979) 373.
- [37] J. V. Geagea *et al.*, Phys. Rev. Lett. **45** (1993) 1980; A. Gillitzer *et al.*, Z. Phys. **A354** (1996) 3.
- [38] S. V. Boyarinov *et al.*, Sov. J. Nucl. Phys. **46** (1987) 871.
- [39] J. B. Carroll *et al.*, Phys. Rev. Lett. **62** (1989) 1829; A. Shor *et al.*, Phys. Rev. Lett. **63** (1989) 2192; A. Schröter *et al.*, Z. Phys. **A350** (1994) 101.
- [40] A. Shor, V. Perez-Mendez and K. Ganezer, Nucl. Phys. **A514** (1990) 717.
- [41] A comprehensive review of the early fixed target data may be found in G. A. Schuler, CERN-TH.7170/94, hep-ph/9403387.
- [42] A. Sansoni, Talk at the 6th International Symposium on Heavy Flavour Physics, Pisa, 6-11 June 1995, Fermilab-Conf-95/263-E, Nuovo Cim. **A109** (1996) 827.
- [43] M. L. Mangano, Talk at Xth Topical Workshop on Proton-Antiproton Collider Physics, Batavia, May 1995, Published in Batavia Collider Workshop 1995, p. 120, hep-ph/9507353.
- [44] T. Matsui and H. Satz, Phys. Lett. **178B** (1986) 416; D. Kharzeev, C. Lourenço, M. Nardi and H. Satz, CERN-TH/96-328, hep-ph/9612217.
- [45] A discussion of hard lepton scattering near threshold may be found in L. L. Frankfurt and M. Strikman, Phys. Rep. **160** (1988) 235.
- [46] U. Camerini *et al.*, Phys. Rev. Lett. **35** (1975) 483.
- [47] B. Gittelman *et al.*, Phys. Rev. Lett. **35** (1975) 1616.
- [48] H. Fritzsche, Phys. Lett. **B67** (1977) 217; F. Halzen, Phys. Lett. **B69** (1977) 105.
- [49] E687 Collaboration, P. L. Frabetti *et al.*, Phys. Lett. **B316** (1993) 197.
- [50] M. G. Ryskin, Z. Phys. **C57** (1993) 89; S. J. Brodsky, L. Frankfurt, J. F. Gunion, A. H. Mueller and M. Strikman, Phys. Rev. **D50** (1994) 3134, hep-ph/9402283.

- [51] ZEUS Collaboration, M. Derrick *et al.*, Phys. Lett. **B350** (1995) 120.
- [52] H1 Collaboration, S. Aid *et al.*, Nucl. Phys. **B472** (1996) 3, hep-ex/9603005.
- [53] M. G. Ryskin, R. G. Roberts, A. D. Martin and E. M. Levin, DTP/95/96, hep-ph/9511228.
- [54] R. Gavai, D. Kharzeev, H. Satz, G. A. Shuler, K. Sridhar and R. Vogt, Int. J. Mod. Phys. **A10** (1995) 3043, hep-ph/9502270.
- [55] G. A. Schuler, CERN-TH/95-75, hep-ph/9504242.
- [56] J. A. Amundson, O. Éboli, E. Gregores and F. Halzen, Phys. Lett. **B372** (1996) 127, hep-ph/9512248; and MADPH-96-942, hep-ph/9605295.
- [57] G. A. Schuler and R. Vogt, Phys. Lett. **B387** (1996) 181, hep-ph/9606410.
- [58] J. H. Kühn, Phys. Lett. **89B** (1980) 385; C. H. Chang, Nucl. Phys. **B172** (1980) 425; E. L. Berger and D. Jones, Phys. Rev. **D23** (1981) 1521; R. Baier and R. Rückl, Phys. Lett. **102B** (1981) 364 and Z. Phys. **C19** (1983) 251; J. G. Körner, J. Cleymans, M. Karoda and G. J. Gounaris, Nucl. Phys. **B204** (1982) 6.
- [59] E. Braaten and T. C. Yuan, Phys. Rev. Lett. **71** (1993) 1673; R. M. Godbole, D. P. Roy and K. Sridhar, Phys. Lett. **B373** (1996) 328, hep-ph/9511433.
- [60] M. Krämer, J. Zunft, J. Steegborn and P. M. Zerwas, Phys. Lett. **B348** (1995) 657; M. Krämer, Nucl. Phys. **B459** (1996) 3.
- [61] M. Cacciari and M. Krämer, Phys. Rev. Lett. **76** (1996) 4128, hep-ph/9601276; and Talk at Workshop on Future Physics at HERA, Hamburg, 30-31 May 1996, hep-ph/9609500.
- [62] NA14 Collaboration, R. Barate *et al.*, Z. Phys. **C33** (1987) 505 and P. Roudeau, Nuclear Physics (Proc. Suppl.) 7B (1989) 273.
- [63] NMC Collaboration, P. Amaudruz *et al.*, Nucl. Phys. **B371** (1992) 553.
- [64] M. Vanttinen, P. Hoyer, S. J. Brodsky and W.-K. Tang, Phys. Rev. **D51** (1995) 3332.
- [65] C. Biino *et al.*, Phys. Rev. Lett. **58** (1987) 2523; E537 Collaboration, C. Akerlof *et al.*, Phys. Rev. **D48** (1993) 5067.
- [66] M. Cacciari, M. Greco, M. L. Mangano and A. Petrelli, Phys. Lett. **B356** (1995) 553, hep-ph/9505379.

- [67] J. L. Cortes and B. Pire, Phys. Rev. **D38** (1988) 3586; B. Pire, Talk at 2nd Meeting on Possible Measurements of Singly Polarized pp and pn Collisions, Int. Rep. Zeuthen-95-05 p. 51, hep-ph/9510454.
- [68] L. Clavelli, P. H. Cox, B. Harms and S. Jones, Phys. Rev. **D32** (1985) 612; J. L. Alonso, J. L. Cortes and B. Pire, Phys. Lett. **B228** (1989) 425.
- [69] G. T. Bodwin, E. Braaten and G. P. Lepage, Phys. Rev. **D51** (1995) 1125.
- [70] E. Braaten and S. Fleming, Phys. Rev. Lett. **74** (1995) 3327, hep-ph/9411365; P. Cho and A. K. Leibovich, Phys. Rev. **D53** (1996) 150, hep-ph/9505329 and Phys. Rev. **D53** (1996) 6203, hep-ph/9511315.
- [71] E. Braaten, S. Fleming and T. C. Yuan, OHSTPY-HEP-T-96-001, hep-ph/9602374.
- [72] J. Amundson, S. Fleming and I. Maksymyk, UTTG-10-95, hep-ph/9601298; P. Ko, J. Lee and H. S. Song, Phys. Rev. **D54** (1996) 4312, hep-ph/9602223.
- [73] M. L. Mangano and A. Petrelli, Talk at the Quarkonium Physics Workshop, Chicago, June 13-15 1996, CERN-TH-96-293, hep-ph/9610364; P. Ernström, L. Lönnblad and M. Vanttinen, NORDITA-96-78-P, hep-ph/9612408.
- [74] W.-K. Tang and M. Vanttinen, Phys. Rev. **D53** (1996) 4851, hep-ph/9506378 and Phys. Rev. **D54** (1996) 4349, hep-ph/9603266.
- [75] M. Beneke and I. Z. Rothstein, Phys. Rev. **D54** (1996) 2005 and **D54** (1996) 7082 (E), hep-ph/9603400.
- [76] S. Gupta and K. Sridhar, Phys. Rev. **D54** (1996) 5545, hep-ph/9601349; and TIFR-TH-96-48, hep-ph/9608433.
- [77] CDF Collaboration, F. Abe *et al.*, Phys. Rev. Lett. **75** (1995) 4358.
- [78] P. Hoyer, talk published in 'Confinement Physics: Proc. 1st ELFE Summer School', Eds. S.D. Bass and P.A.M. Guichon (Editions Frontieres, 1996), p.343, hep-ph/9511411.
- [79] E772 Collaboration, D. M. Alde *et al.*, Phys. Rev. Lett. **64** (1990) 2479.
- [80] G. A. Alves *et al.*, Phys. Rev. Lett. **70** (1993) 722; M. J. Leitch *et al.*, Phys. Rev. Lett. **72** (1994) 2542.
- [81] J. Badier *et al.*, Z. Phys. **C20** (1983) 101; S. Katsanevas *et al.*, Phys. Rev. Lett. **60** (1988) 2121; D. M. Alde *et al.*, Phys. Rev. Lett. **66** (1991) 133 and 2285; M. J. Leitch *et al.*, Nucl. Phys. **A544** (1992) 197c.
- [82] P. Hoyer, M. Vanttinen and U. Sukhatme, Phys. Lett. **B246** (1990) 217.

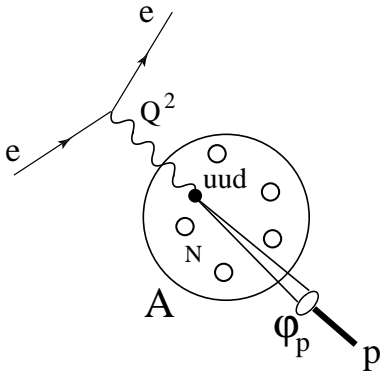
- [83] S. J. Brodsky, P. Hoyer, C. Peterson and N. Sakai, Phys. Lett. **B93** (1980) 451; S. J. Brodsky, C. Peterson and N. Sakai, Phys. Rev. **D23** (1981) 2745.
- [84] R. Vogt, S. J. Brodsky and P. Hoyer, Nucl. Phys. **B360** (1991) 67.
- [85] S. J. Brodsky and P. Hoyer, Phys. Lett. **B298** (1993) 165.
- [86] P. Jain and J. P. Ralston, KANSAS-94-5-22, hep-ph/9406394.
- [87] E691 Collaboration, M. D. Sokoloff *et al.*, Phys. Rev. Lett. **57** (1986) 3003.
- [88] J. Hüfner, B. Kopeliovich and A. B. Zamolodchikov, MPI-H-V26-1996, nucl-th/9607033.
- [89] K. Adel and F.J. Yndurain, Phys. Rev. **D52** (1995) 6577, hep-ph/9502290; J. Smith and R. Vogt, ITP-SB-96-60, hep-ph/9609388.
- [90] EMC Collaboration, J. J. Aubert *et al.*, Nucl. Phys. **B213** (1983) 31; E. Hoffmann and R. Moore, Z. Phys. **C20** (1983) 71; B.W. Harris, J. Smith and R. Vogt, Nucl. Phys. **B461** (1996) 181, hep-ph/9508403.
- [91] R. Vogt and S. J. Brodsky, Phys. Lett. **B349** (1995) 569, hep-ph/9503206
- [92] A. D. Krisch, Nucl. Phys. B (Proc. Suppl.) **25** (1992) 285.
- [93] S. J. Brodsky and G. F. de Teramond, Phys. Rev. Lett. **60** (1988) 1924.
- [94] S. J. Brodsky, G. F. de Teramond and I. A. Schmidt, Phys. Rev. Lett. **64** (1990) 1011.
- [95] M. Luke, A. V. Manohar and M. J. Savage, Phys. Lett. **B288** (1992) 355.
- [96] O. Nachtmann, Johns Hopkins Workshop 1994:143-172, hep-ph/9411345.
- [97] D. Diakonov, Talk at International School of Nuclear Physics, Erice, Italy, Sept. 1995, nucl-th/9603023.
- [98] P. Hoyer, NORDITA-96/63 P, hep-ph/9610270.

EXCLUSIVE

$$e A \rightarrow e p (A-1)$$

$$\sigma = F_{p/A} * |\Phi_p|^2$$

- * $\hat{\sigma} [e (uud) \rightarrow e (uud)]$
- * Transparency * $|\Phi_p|^2$



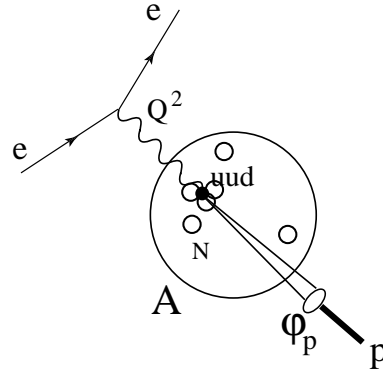
- Nucleus \approx ground state
- Compact uud belongs to a single nucleon

SEMI - INCLUSIVE

$$e A \rightarrow e p X$$

$$\sigma = F_{uud/A}$$

- * $\hat{\sigma} [e (uud) \rightarrow e (uud)]$
- * Transparency * $|\Phi_p|^2$



- Excited nuclear state
- Compact uud can originate in a multi-nucleon cluster

Figure 5: Comparison of proton knock-out from nuclei in the exclusive $eA \rightarrow ep(A-1)$ process and a semi-inclusive one, $eA \rightarrow epX$ with $z = E_p/\nu \rightarrow 1$. The latter can have contributions from highly excited nuclear states containing compact multinucleon clusters.

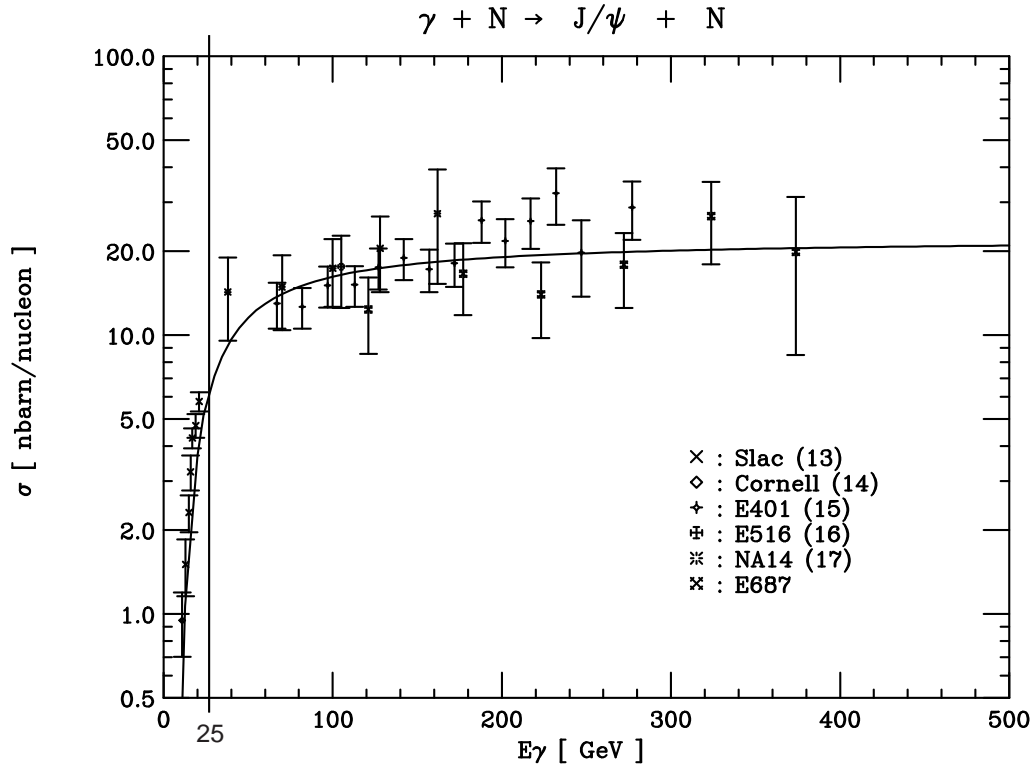


Figure 6: Compilation of cross sections for the process $\gamma p \rightarrow J/\psi p$ [49]. Experiments at ELFE will be in the range $E_\gamma \lesssim 25$ GeV (vertical line). The curve shows the prediction of Eq. (13) for a gluon structure function $xG(x) = 3(1-x)^5$.

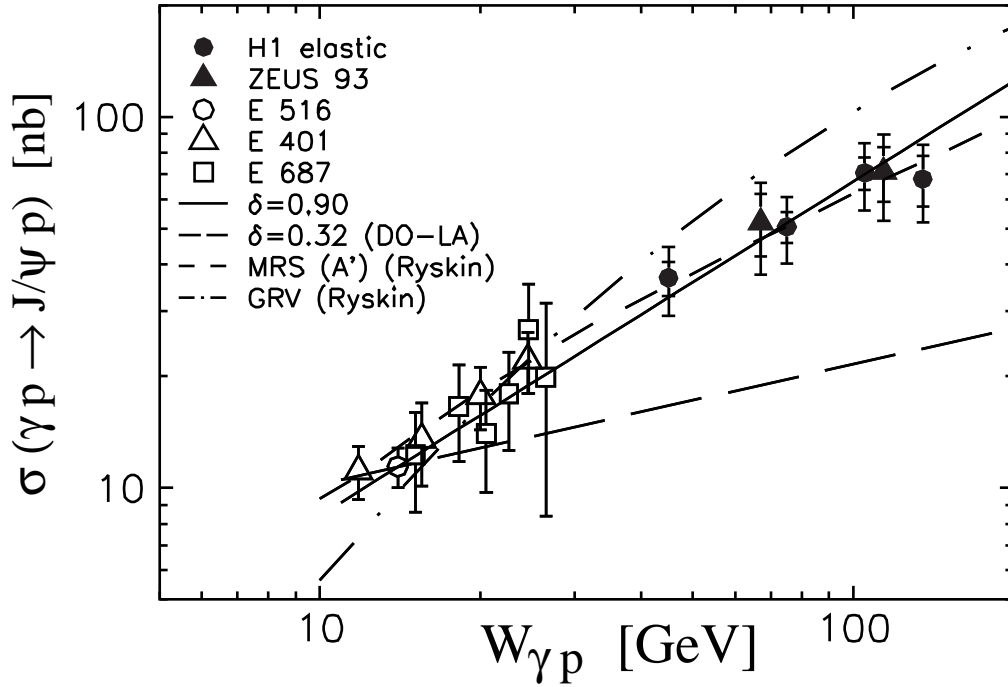


Figure 7: Compilation of high energy data on the process $\gamma p \rightarrow J/\psi p$ [52], with curves of the form $W_{\gamma p}^{\delta}$ as indicated. The curves marked ‘MRS’ and ‘GRV’ are the results of QCD calculations with two-gluon exchange [50, 53], for different gluon structure functions.

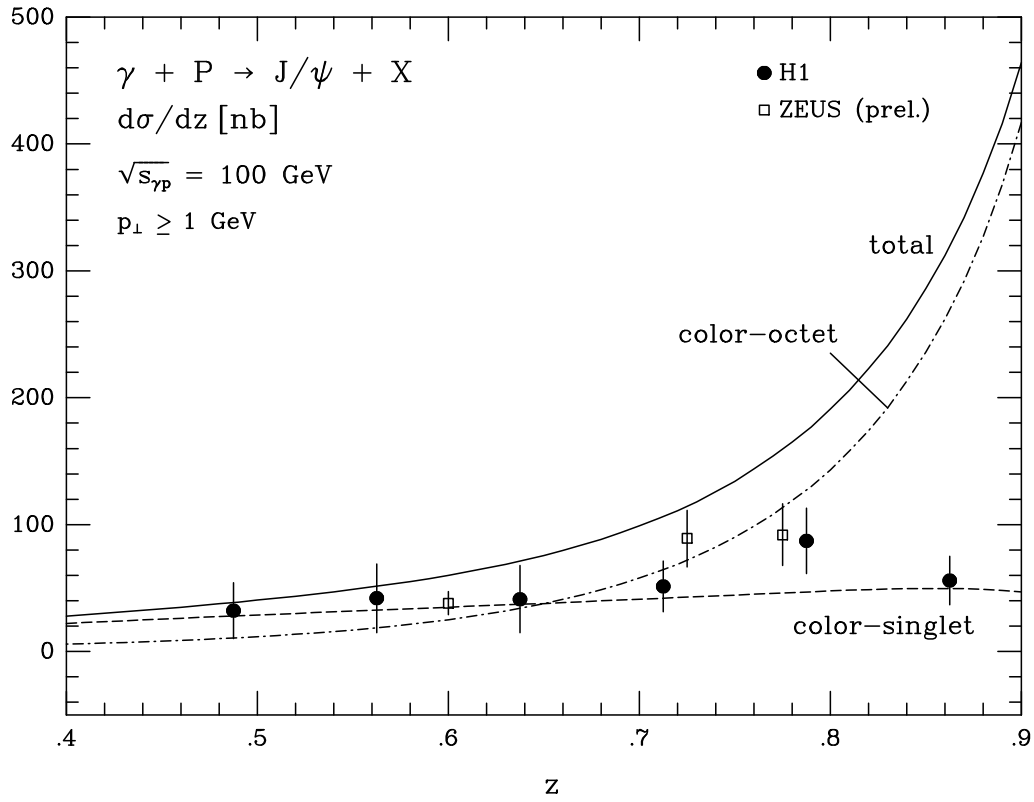


Figure 8: The cross section for inelastic J/ψ photoproduction $\gamma p \rightarrow J/\psi + X$ for $p_{\perp}(J/\psi) \geq 1$ GeV as a function of the J/ψ energy fraction (in the proton rest frame) $z = E_{J/\psi}/E_{\gamma}$ [61]. Predictions based on the color singlet and octet mechanisms are compared to data from HERA.

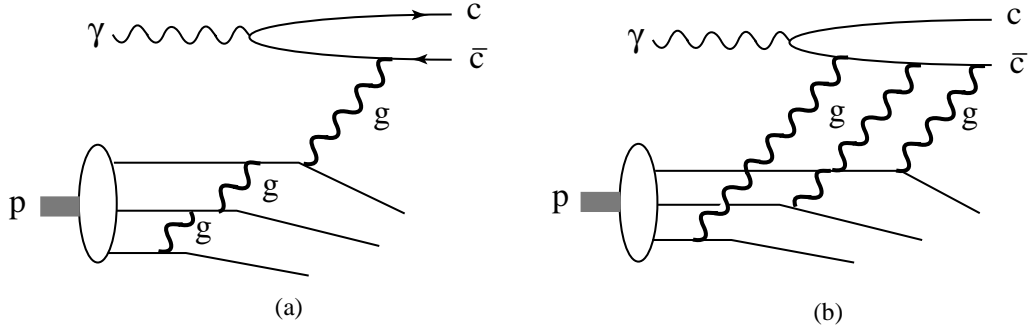


Figure 9: Two mechanisms for transferring most of the proton momentum to the charm quark pair in $\gamma p \rightarrow c\bar{c} + X$ near kinematic threshold. The leading twist contribution (a) dominates at high energies, but becomes comparable to the higher twist contribution (b) close to threshold.

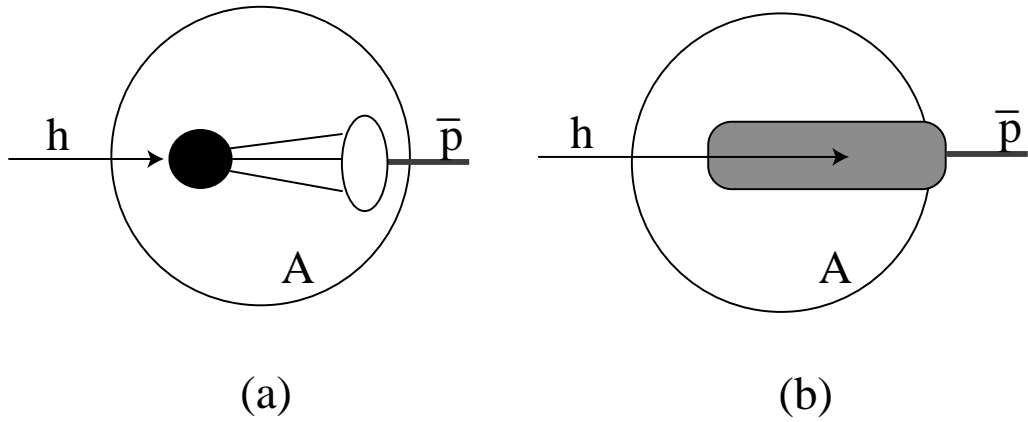


Figure 10: Two conceptual mechanisms for subthreshold \bar{p} production in hA collisions. In (a) the production occurs locally off a hot spot (black circle) of high energy density in the nucleus. In (b) the light quarks gain momentum over an extended nuclear region (grey).